Effect of Packing and Tilt on the Rotational Barriers of an Amino, Nitro-Substituted Phenylene Ethynylene Trimer

Alessandra Ricca* and Charles W. Bauschlicher, Jr.

Mail Stop 230-3, Center for Nanotechnology, NASA Ames Research Center, Moffett Field, California 94035

Received: September 29, 2004; In Final Form: February 24, 2005

Rotational potentials are computed for heptamers and nonamers of an amino, nitro-substituted phenylene ethynylene trimer molecule. A herringbone and a parallel-slipped packing arrangement are considered. The effect of tilting the molecules with respect to the surface as well as the effect of the gold support are also taken into account. The herringbone structure with the molecules perpendicular to the surface has a low rotational barrier (2 kcal/mol). Tilting the molecules by 30° increases the rotational barriers significantly (16 kcal/mol). The parallel-slipped structure has rotational barriers of 7 kcal/mol. Including the effect of the gold support increases the rotational barriers for tilted molecules but has little effect on perpendicular molecules.

I. Introduction

A self-assembled monolayer (SAM) of a conjugated phenylene ethynylene trimer on Au(111) containing an amino and a nitro group in the central ring has attracted considerable attention because of a very sharp negative differential resistance (NDR) observed at 60 K.[1] Using the same molecule, Reed et al.[2] demonstrated that they could read, write, and erase data with the application of voltage pulses. The bit retention decreases exponentially in time and varies depending on the phenyl ring substituents.[3] On the basis of the change in retention time with temperature, an activation energy of 1.8 kcal/mol was obtained. Such an activation energy is very low and consistent with the rotational barriers of the phenyl rings. In our previous work,[4] we computed the rotational barriers for a single phenylene ethynylene trimer containing an amino and a nitro group, and we showed that the barriers for the anions were consistent with the measured retention times whereas the barriers for the cations and the neutral molecules were not. Our calculations were based on the assumption that packing would affect the rotational barriers of the rings having the largest substituents but would have a small effect on the rotational barriers of the remaining rings. In the present paper, we want to assess how packing affects the rotational barriers of each of the phenyl rings.

Despite the interest in SAMs of phenylene ethynylene oligomers, their packing on Au(111) is not completely elucidated. For an unsubstituted phenylene ethynylene trimer, Sita and co-workers[5] observed a commensurate structure using scanning tunneling microscopy (STM) in air at room temperature. Subsequently, Sita and co-workers,[6] using higher resolution images produced by an STM under ultrahigh vacuum, concluded that the unsubstituted trimers form incommensurate SAMs on Au(111). They observed that phenyl rings arranged in a herringbone fashion with the molecules only slightly tilted with respect to the surface normal. Dholakia et al.[7] also concluded that unsubstituted trimers form incommensurate SAMs on Au(111) using STM under vacuum. Our previous theoretical calculations[8,9] showed that the binding energy did not vary significantly with the position of the S on the Au surface, which is consistent with the formation of incommensurate SAMs, that is, if the binding is independent of the position of the S on the metal surface, the molecule−molecule interactions determine the packing. We also suggested that at low coverage the arene thiol oligomers should be bent whereas at high coverage they should be perpendicular to the surface.

Recently, Stapleton et al.[10] prepared a SAM of the unsubstituted trimer, and they deduced a tilt angle of 33° from the surface normal using infrared spectroscopy. They also prepared a nitro-substituted trimer and obtained a well-ordered commensurate SAM with a molecular tilt angle of 32−39°. However, a detailed picture of the structure of the SAM did not emerge because of the lack of resolution of the atomic force microscopy (AFM) technique used. Using an STM, Walzer et al.[11] did not observe any molecular order in the structure of the SAM of a nitro-substituted trimer. We are unaware of any characterization of the SAM of an amino, nitro-substituted phenylene ethynylene trimer. Overall, the information provided by experiment on SAMs of nitro-substituted phenylene ethynylene trimers is not conclusive which must be due in large part to the extreme difficulty in preparing the SAMs.

In our study, we assume that amino, nitro-substituted phenylene ethynylene trimers form incommensurate SAMs on the basis of our previous theoretical work and on the conclusive experiments on unsubstituted phenylene ethynylene trimers. We also assume that an ordered SAM can be obtained.

II. Methods

All calculations are carried out using the hybrid[12] B3LYP[13] functional. For the Au atoms, we use the LANL2DZ and LANL2MB[14] basis sets and their associated electron−core potentials (ECPs). For the remaining atoms, we use two basis sets:[15] the small set is 4-31G on all of the atoms, while the large set is 6-31G* for C and H and 6-31+G* for S. All the calculations were performed using the program Gaussian 03.[16]

We first study the effect of tilting the molecule with respect to the surface on the rotational barrier of the phenyl ring of a benzene and of a $S-C_6H_5$ molecule bound to a cluster of Au atoms which simulates the (111) face of Au. The positions of the Au atoms are taken from data for bulk gold. The H or S atoms are directly above a threefold hollow (see Figure 1), where

* Author to whom correspondence should be addressed.

10.1021/jp045572a CCC: $30.25
Published on Web 04/02/2005

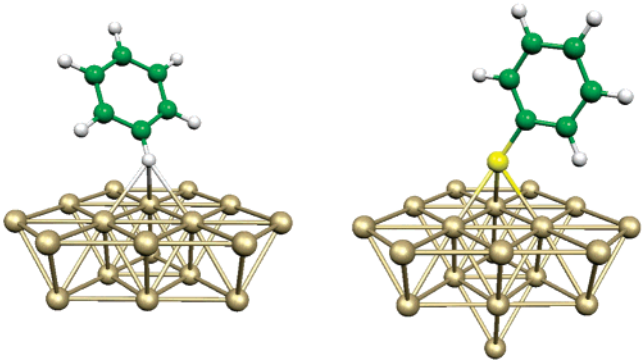

Figure 1. The models used to study the rotation of benzene and SC_6H_5 above a Au(111) surface.

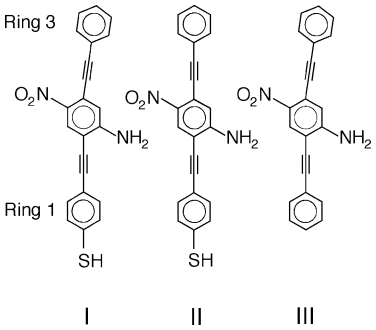

Figure 2. The three models for the amino, nitro-substituted trimer.

the three Au atoms are described using the LANL2DZ basis set, while the remaining Au atoms use the LANL2MB set. The benzene and $S-C_6H_5$ are described using the large basis set. The cluster used for $S-C_6H_5$ has one more Au atom than that used for the benzene calculation; this is to make both systems closed shells. The rotation of the C_6 ring about the C−H or C−S bonds are considered for both a ring perpendicular and a ring tilted with respect to the surface. The ultrafine grid is used in these calculations since some of the rotational potentials are very flat.

In a second set of calculations, we focus on the effect of tilting and packing on the rotational barriers of models of an amino, nitro-substituted phenylene ethynylene trimer using the three different molecules shown in Figure 2. The gold support is not taken into account in our calculations because of the large size of our models. The effect of the gold support is studied using the models shown in Figure 1. Because of the size of the system, excluding a calibration calculation, only the small basis set is used in these studies. The molecules labeled I and III in Figure 2 differ in the terminal group at one end of the molecule, namely, SH versus H. They are fully optimized at the B3LYP/4-31G level of theory. The repulsion from the NO_2 group causes a small bend of the adjacent terminal −C≡C− unit. Since the energy associated with this bend is small and of approximately the same magnitude as the intermolecular forces involved in the SAM, we also optimize model II with the constraint that all the carbon atoms of the two C−C≡C−C units lie on a line. To study the effect of packing, we surround molecules I−III with six and eight identical molecules to produce, respectively, a heptamer and a nonamer. The rotational potentials are computed for the three phenyl rings of the molecule in the center of the arrangement to avoid artifacts from edge effects. We study the effect of the Au−S−C tilt angle by comparing the rotational barriers for the molecules perpendicular to the surface with those for the molecules tilted by an angle of 30°. A detailed description of the various packing arrangements considered in this work is given in the next section. For each packing model, we optimize the relative arrangement of the seven or nine frozen molecules. The parameters that are optimized are discussed in detail in the next section for each model separately.

The calculation of the rotational barriers is very computationally demanding even using the 4-31G basis set, but such a small basis set can yield computational artifacts. Therefore, we perform one calibration calculation of a rotational potential for one ring using a larger basis set, namely, 6-31++G* on all the atoms except the carbons, which use a 6-31G* basis set. The diffuse functions are not included on the carbons since this leads to many functions being deleted to avoid linear dependencies. The result for the larger basis set, shown below, supports the use of the smaller basis set.

III. Results and Discussion

A. C_6H_5X (X = H, S) on an Au Cluster. In the first series of calculations, the C_2 axis of the SC_6H_5 and the analogous axis in benzene is constrained to be perpendicular to the Au surface. The height above the surface (R) is optimized for SC_6H_5 and the rotational potential is computed for $R = 2.185$ Å above a threefold hollow site. The barrier in the rotational potential is less than 0.02 kcal/mol. This is still true even if R is reduced to 1.8 Å. The potential for the height of benzene above a threefold hollow site of the gold surface is quite flat until the H is at about 2.0 Å above the surface. We compute the rotational barrier for the H heights above the surface ranging from 2.7 to 1.4 Å, and for all values the rotational barrier is less than about 0.1 kcal/mol. Thus, we conclude that for either the S end or the H end interacting with the Au surface, there is no significant rotational barrier if the molecule is perpendicular to the Au surface.

If we optimize the $Au_{19}SC_6H_5$ model, with the positions of the Au atoms frozen and the S is fixed above the threefold hollow, we find a minima, where one of the H atoms tilts toward the surface, with a surface−S−C angle (A) of 146.2° and the surface−S distance (R) of 2.26 Å. The rotation of the C_6H_5 about the S−C axis yields a small barrier. If R is reduced to 2.0 Å, the rotational barrier is still only about 0.4 kcal/mol. Further increasing the tilt angle A to 135.0° for $R = 2.0$ Å yields a barrier of slightly more than 7 kcal/mol. For a tilt angle of 135°, but at $R = 2.26$ Å, the barrier is 2.8 kcal/mol. Therefore, while there is only a very small barrier for tilts away from perpendicular up to about 34°, the barrier can become sizable for larger tilts, provided the bond length is shorter than that optimized.

Finally, tilting the face of the benzene toward the surface can produce much larger tilt angles (see refs 8, 9) for single molecules on the surface. However, this situation is unlikely to occur for SAMs.

For benzene, we consider surface−H distances (R) of 1.8 and 2.0 Å and a tilt of 30° away from perpendicular, and we find a barrier of about 12 and 8 kcal/mol, respectively. Thus, the case of the H-end interacting with the metal appears to have larger barriers because the ring approaches the surface more closely. That is, the S atom holds the ring further away from the surface and hence leads to lower barriers. Thus, a tilted molecule with S atoms on both ends might act differently from one with a S atom on one end and a H atom on the other as the H end would be expected to have a sizable rotational barrier.

B. Packing of Amino, Nitro-Substituted Trimers. *1. Heptamers.* We first consider a heptamer with a herringbone structure and with the molecules perpendicular to the surface. The geometrical parameters optimized for molecules I and II

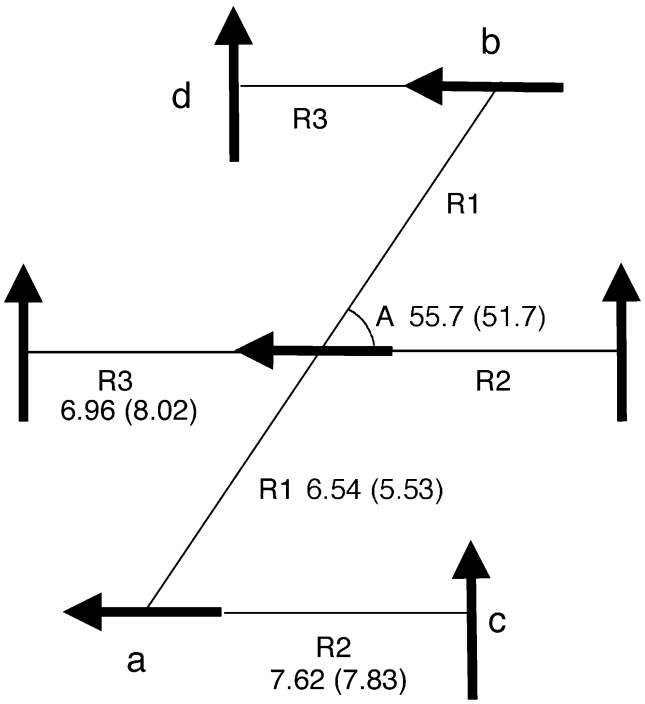

Figure 3. Herringbone structure for a heptamer of molecule I and II. The geometrical parameters optimized for molecule I and II are shown in the figure. The values given in parentheses are for molecule II. The arrow indicates the side with the NO_2 group.

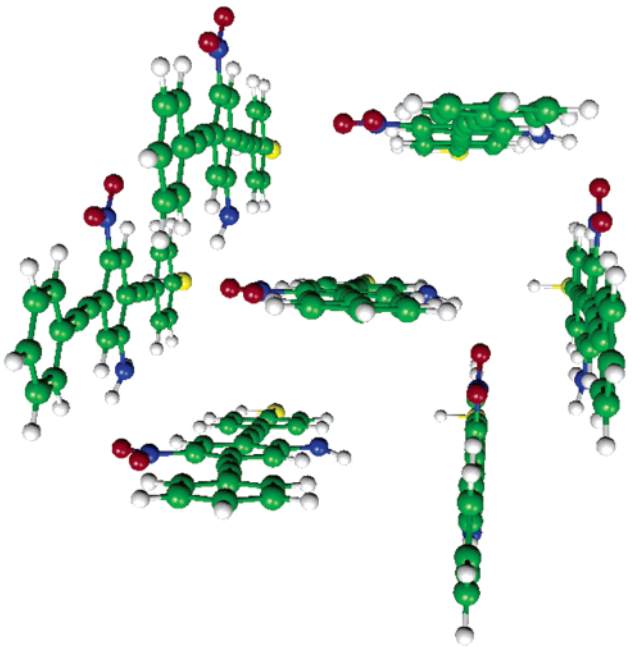

Figure 4. The optimized structure for a heptamer of molecule I arranged in a herringbone structure. The molecules are perpendicular to the surface.

are shown in Figure 3. The optimized structure for the heptamer of molecule I is shown in Figure 4, and the rotational potentials for molecules I and II are shown in Figures 5 and 6, respectively. For molecule I, the rotational potentials of ring 1 (the C_6H_4 ring adjacent to the SH group) and ring 3 (the terminal C_6H_5) have somewhat similar shapes with the same maxima but with the lowest minima shifted by 40°. For molecule II, the two curves have almost identical shapes and are parallel to each other. By imposing the constraint that the two C−C≡C−C units lie on a line, ring 1 and ring 3 of molecule II are equidistant

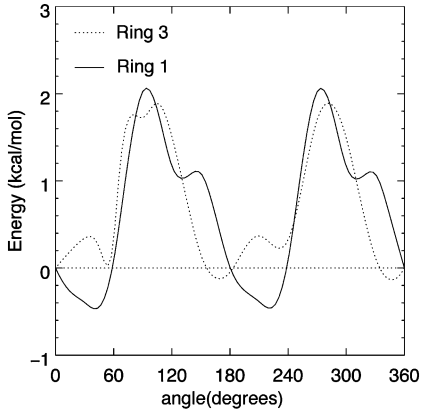

Figure 5. Rotational potentials for a herringbone structure of a heptamer composed of molecule I. The molecules are perpendicular to the surface. A positive angle is defined to be a rotation in the counterclockwise direction.

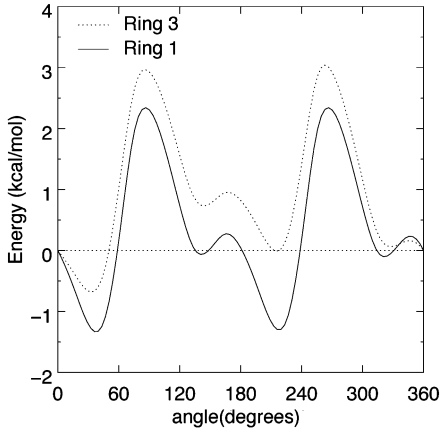

Figure 6. Rotational potentials for a herringbone structure of a heptamer composed of molecule II. The molecules are perpendicular to the surface.

from adjacent aromatic rings and the rotational potentials for rings 1 and 3 are parallel. However, because of the asymmetry introduced by the amino and nitro groups, rings 1 and 3 do not experience identical intermolecular and intramolecular forces and their curves are not identical but slightly shifted in energy. Two sets of minima are present in every case for ring 1. One set is for angles of 45° and 225° which is lower in energy and another set is for angles of 135° and 315°. Calculations performed including only ring 1 thiol surrounded by six other identical ring 1 thiols in a herringbone arrangement show that the conformation with an angle of 45° is the lowest in energy followed by the planar and then the one with an angle of 135°. The energy difference between the conformation with an angle of 45° and the one with an angle of 135° is 1.41 kcal/mol, and the energy difference between the planar conformation and that with an angle of 45° is only 0.96 kcal/mol. Overall, the rotational potential can be explained mainly by the intermolecular interactions between ring 1 and its adjacent ring 1 molecules. For angles of 45° and 225°, ring 1 lies on a line connecting molecules a and b (see Figure 3) and is in a slipped T-shape configuration with respect to rings in molecules a and b. The hydrogen atoms of ring 1 point toward the center of adjacent rings. For angles of 135° and 315°, ring 1 lies on a line connecting molecules c and d. The 135° and 315° conformations appear to be less stable than the 45° and 225° ones as the hydrogens of ring 1 do not point directly toward the center of adjacent rings and experience more repulsion with adjacent H

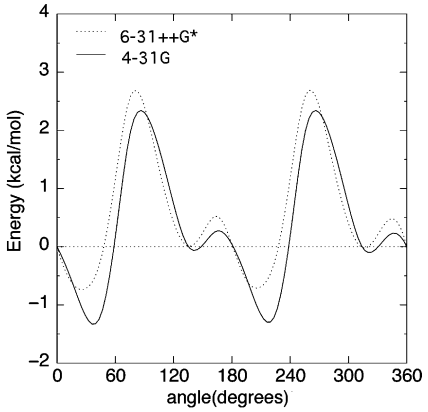

Figure 7. Ring 1 rotational potentials for a herringbone structure of a heptamer composed of molecule II for the small and large basis set. The small basis set results are the same as those in Figure 6.

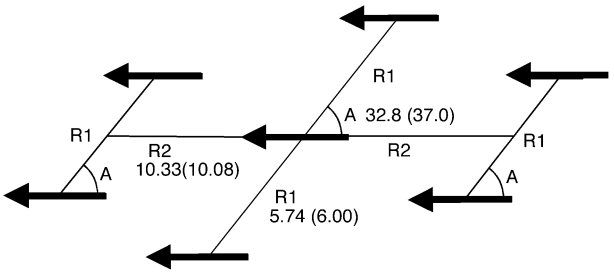

Figure 8. The parallel-slipped structure for a heptamer of molecule II. The geometrical values shown in the figure are optimized for molecules perpendicular to the surface, and the values given in parentheses are for molecules tilted by 30° with respect to the surface. The arrow indicates the side with the NO_2 group.

atoms. To confirm that the slipped T-shape conformation is not an artifact due to basis set superposition error (BSSE), we compute the BSSE for ring 1 in the heptamer of molecule I. The BSSE for the planar case is 3.40 kcal/mol whereas for the 45° rotation the BSSE is 3.30 kcal/mol. Clearly, BSSE cannot explain why the rotated conformation is more stable. The largest rotational barrier is in the range of 2.5−3.5 kcal/mol which is clearly small.

In addition to computing the BSSE for molecule I, we compute the rotational potential for ring 1 of molecule II using the larger 6-31++G* basis set which is compared to the rotational potential for the small 4-31G basis set in Figure 7. While there are some differences between the two potentials, overall the agreement is very good, with all the structure of the rotational potential computed using the smaller basis set reproduced using the larger basis set. Thus, the larger basis set supports the use of the smaller set for the overall features of the rotational potential; however, one must realize that the barriers computed using the 4-31G basis set have some uncertainty.

The rotational potential of ring 3 in the heptamer of molecule I is similar to that of a phenyl ring in the isolated amino, nitro-substituted trimer molecule with the lowest minima around 0° and 180° and a rotational barrier of 2 kcal/mol. The tilt of the C−C≡C−C unit in molecule I increases the distance between ring 3 and its adjacent neighbors and reduces the intermolecular interactions to such an extent that ring 3 behaves like a free ring. We do not show the rotational potentials of ring 2 as the rotational barrier to rotate this ring is very high because of the steric repulsion introduced by the presence of the NO_2 and NH_2 substituents. In the herringbone structure shown in Figure 3, ring 2 of the central molecule is clearly in a stable planar conformation. The slight rotation of ring 1 could be a true minimum indicating that ring 1 and ring 3 are not coplanar or it could be because our herringbone structure does not minimize the intermolecular interactions of ring 1. However, the energy difference between the coplanar and the rotated conformation is very small, being less than 1.5 kcal/mol.

We next consider a heptamer with a parallel-slipped structure, and we only consider molecule II. The geometrical parameters optimized are shown in Figure 8 and the optimized structure in Figure 9. For this system, we consider the case where the molecules are perpendicular to the surface and also the case where the face of the benzene ring tilts toward the surface. In the tilted case, we fix the surface−S−C angle at 30° and optimize the geometrical parameters shown in the figure. The rotational potentials are shown in Figures 10 and 11. The rotational potential for molecule II perpendicular to the surface, shown in Figure 10, has two minima around 0° and 180° and two maximas for angles of 60° and 240°. The curves for ring 1 and ring 3 are almost superimposed as for the case of molecule II in a herringbone conformation (see Figure 6). For rotational angles of 60° and 240°, the hydrogens of ring 1 are at only 2 Å from neighboring hydrogens and the repulsion reaches its maximum. Planar conformations minimize the repulsion between the hydrogen atoms. The barrier height of 7 kcal/mol, which is larger than the barrier of 2.5−3.5 kcal/mol for the herringbone conformation, indicates that the parallel-slipped conformation is more effective at locking the rings in a planar conformation. Calculations performed using only ring 1 of the molecule surrounded by six other single rings in a parallel-slipped conformation with the molecules perpendicular to the surface also show that the planar conformation is the lowest in energy with maximas for 60° and 240°. The barrier of rotation is computed to be 5.42 kcal/mol. Adding a C−C≡C−C unit with ring 2 attached to it does not affect the position of the peaks but slighlty increases the barrier to a value of 6.25 kcal/mol.

Tilting molecule II by 30° with respect to the surface introduces a sliding of the rings with respect to each other and the interactions of ring 1 with its neighbors are different from those of ring 3. As a result, the curves for the two rings are slightly shifted both in angle and energy. However, the changes are minor and the minima are still around 0° and 180° and the maximas are around 60° and 240°. The rotational barriers are between 4 and 5 kcal/mol, which is 2 kcal/mol smaller than for the perpendicular case. For the tilted case, the repulsion between hydrogen atoms in adjacent rings reaches its maximum for a rotational angle of 60° and 240° as for the perpendicular case. However, the distance between the hydrogens for the rotation of 60° is 2.70 Å versus 2.0 Å for the perpendicular case. Therefore, the rotational barrier is lower for the tilted case. If a Au surface is included in the model for the tilted case, the barrier should increase and could be similar to that for the perpendicular case. Calculations performed using only ring 1 thiol surrounded by six other identical ring 1 thiols in a parallel-slipped conformation with the molecules tilted by 30° are consistent with the results described above. The rotational barrier is computed to be 3.15 kcal/mol. Adding an extra C−C≡C−C unit with ring 2 attached to it increases the barrier to a value of 3.65 kcal/mol. Using only ring 1 in the parallel-slipped heptamer captures a significant fraction of the intermolecular interactions involved.

2. Nonamers. In this subsection, we study the effect of having two additional molecules surrounding a central molecule by

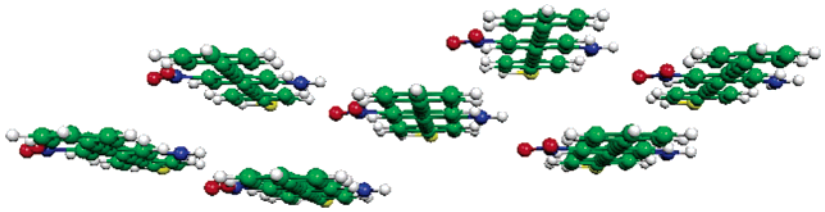

Figure 9. The optimized structure for a heptamer of molecule II arranged in a parallel-slipped structure. The molecules shown are perpendicular to the surface.

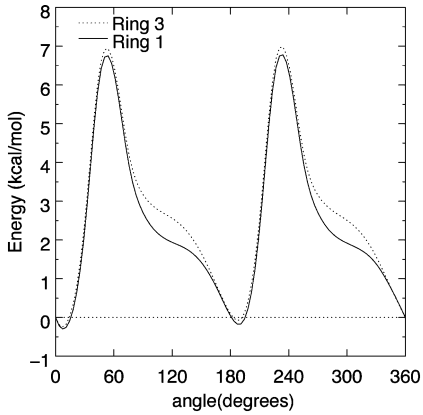

Figure 10. Rotational potentials for a parallel-slipped structure of a heptamer composed of molecule II. The molecules are perpendicular to the surface.

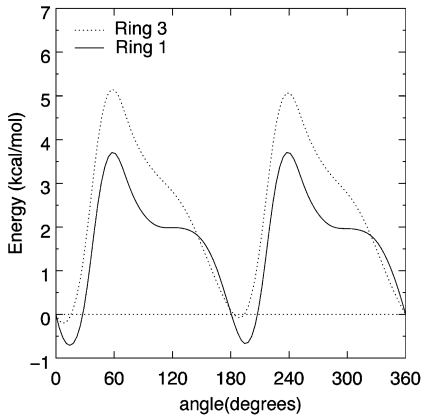

Figure 11. Rotational potentials for a parallel-slipped structure of a heptamer composed of molecule II. The molecules are tilted by an angle of 30° with respect to the surface.

using a nonamer. We consider both the cases of molecules being perpendicular to the surface and tilted by 30° with respect to the surface. We first consider a nonamer composed of molecule III in a herringbone arrangement with the molecules perpendicular to the surface. The geometrical structure and the optimized geometrical parameters are shown in Figure 12. The difference between the herringbone structure for the nonamer and that for the heptamer (see Figure 3) is that for the nonamer we optimize an additional parameter B which removes the restriction that the middle row of molecules lies on the line connecting the bond midpoints of the first and third rows. Optimizing this additional degree of freedom leads to sizable changes in the separation between the central molecule and its neighbors and maximizes the intermolecular hydrogen bonding between the NO_2 group on one molecule and the NH_2 group on the adjacent molecule. The optimized structure is shown in Figure 13 and the rotational potential in Figure 14. Ring 3 of molecule III is tilted as for molecule I, and the rotational potential of ring 3 shown in Figure 14 is very similar to that of

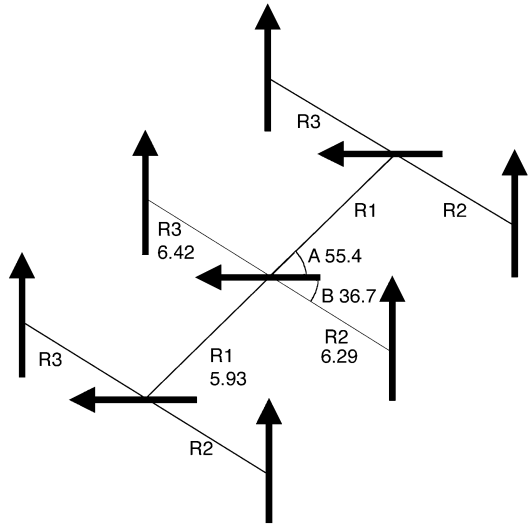

Figure 12. Herringbone structure for a nonamer of molecule III with the molecules perpendicular to the surface. The geometrical parameters optimized are shown in the figure. The arrow indicates the side with the NO_2 group.

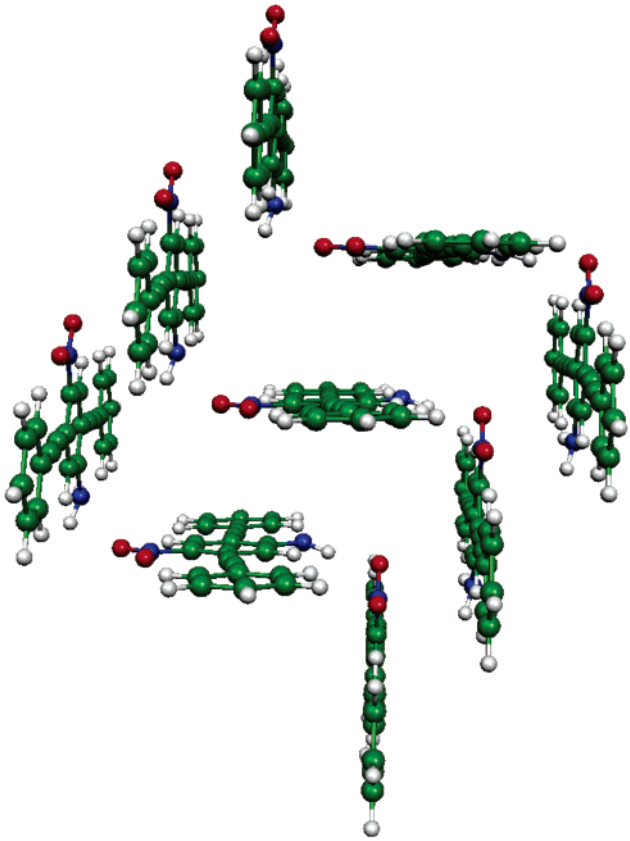

Figure 13. The optimized structure for a nonamer of molecule III arranged in a herringbone structure. The molecules are perpendicular to the surface.

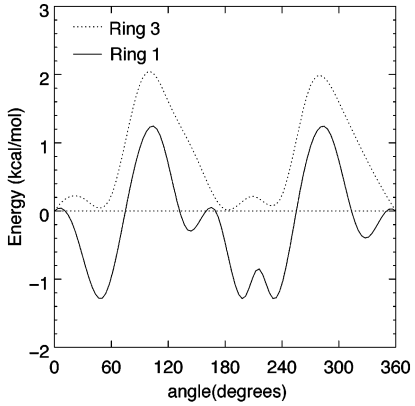

Figure 14. Rotational potentials for a herringbone structure of a nonamer composed of molecule III. The molecules are perpendicular with respect to the surface.

ring 3 shown in Figure 5 with two minima around 0° and 180° and a barrier of 2 kcal/mol. Ring 1 of molecule III has no SH group and is therefore somewhat different than ring 1 of molecule I. In addition, the angle B is optimized for molecule III but not for molecule I, which results in significant changes in the distances between the central molecule and its neighbors. This change in distance results in the central molecule interacting with four neighbors at the same time at some angles, which leads to some extra structure in the rotational potential, such as the small bump at 215°. Nevertheless, the position of the minima at 50° and 140° and a rotational barrier of 2 kcal/mol is very similar to the case of the heptamer. Overall, the rotational potentials of the herringbone nonamer are very similar to those of the herringbone heptamer. Our calculations confirm that including two extra molecules in the packing produces only small changes when the molecules are perpendicular to the surface. Optimizing angle B does not affect much the rotational potentials which indicates that the intermolecular distances between ring 1 and ring 3 with their neighbors are only slightly modified.

We also consider a nonamer composed of molecule II in a herringbone arrangement with a surface−S−C tilt angle of 30°. As optimizing B did not significantly affect the rotational potentials for the herringbone nonamer, we fix the B value to 0° which corresponds to the herringbone structure for the heptamer (see Figure 3). For this herringbone arrangement, it is possible to tilt every other row of molecules in the opposite direction. This type of tilt is different than the one studied for the heptamer of molecule II in a parallel-slipped arrangement. The optimized structure is shown in Figure 15 and the potential is shown in Figure 16. The rotational potentials of both ring 1 and ring 3 show that the planar conformation is by far the most stable. The conformations with a rotational angle of 60° and 240° are higher in energy by 16 kcal/mol. For 60° and 240°, the hydrogen atoms of the rotating ring are at a distance of 1.7 Å from the hydrogen atoms of the adjacent rings in the same central row and the repulsion is very high. This tilted conformation is the conformation which has the highest rotational barrier among the ones we have considered. Including a Au surface in our model should increase our computed rotational barriers. In our models, we have optimized the intermolecular distances and the molecules are as closely packed as possible which should correspond to the case of incommensurate structures. For commensurate structures, the arrangement of the molecules on the gold surface is dictated by the positions of the gold atoms and the molecules are further apart. Therefore, we expect that our computed rotational barriers are higher than those for a commensurate structure and correspond to an upper bound.

Overall, our results indicate that packing and tilting can affect the rotational potentials. We have only considered a few representative packing arrangements, and more are possible. Several packing/tilting combinations could lead to similar rotational potentials. Our smallest rotational barrier has been obtained for a herringbone structure with molecules perpendicular to the surface. The activation energy of 1.8 kcal/mol deduced from experiment by Reed et al. could be consistent with such a structure if incommensurate structures are those obtained experimentally.

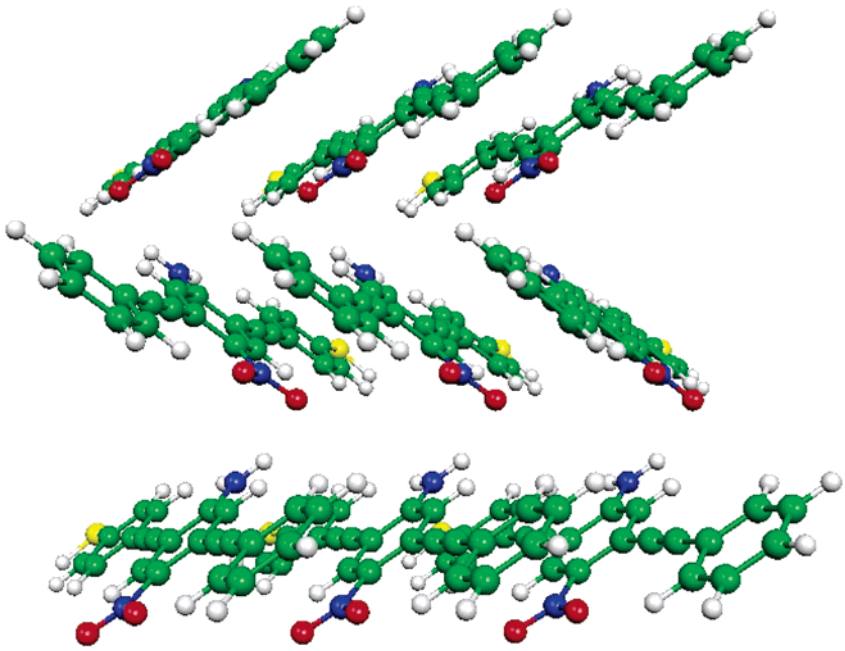

Figure 15. The optimized structure for a nonamer of molecule II arranged in a herringbone structure. The molecules are tilted by an angle of 30° with respect to the surface. The parameters optimized are shown in Figure 12 and the optimized values are $R1 = 5.45$ Å, $R2 = 10.02$ Å, $R3 = 10.94$ Å, and $A = 39.1°$. The angle B is fixed at 0°.

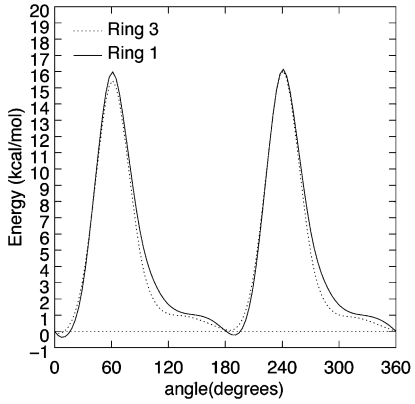

Figure 16. Rotational potentials for herringbone structure of a nonamer composed of molecule II. The molecules are tilted by an angle of 30° with respect to the surface.

IV. Conclusions

We have studied the rotational potentials of two representative packing arrangements, namely, a herringbone and a parallel-slipped arrangements. The geometries of these structures have been optimized in the absence of a gold support and correspond to incommensurate structures.

Our work shows that the presence of a gold surface has no effect on the rotational barriers if the molecules are perpendicular to the surface. If the molecules are tilted and have a H terminal group pointing at the gold surface, the rotational barriers increase significantly. The effect is reduced if the terminal group is a thiol due to an increase in the distance between the surface and the phenyl hydrogens pointing at the surface.

The herringbone structure with the molecules perpendicular to the surface without including a gold support has a low rotational barrier (2 kcal/mol). On the basis of the $Au_{19}SC_6H_5$ calculations, we believe that adding a top and bottom gold surface to the array of molecules will not affect the rotational barriers. Tilting the molecules by an angle of 30° with respect to the surface in the absence of a gold support increases significantly the intermolecular repulsion, and the rotational barriers are high (16 kcal/mol). Adding a top gold layer above ring 3 is expected to increase the barrier by several kcal/mol and adding a bottom layer below ring 1 is also expected to increase the barrier but somewhat less than for ring 3.

The parallel-slipped structure with the molecules perpendicular to the surface without including a gold support has a higher barrier (7 kcal/mol) than the corresponding herringbone structure. Tilting the molecules by an angle of 30° in the absence of gold reduces by 2 kcal/mol the barrier due to an increase in the intermolecular distances. However, as for the herringbone case, the $Au_{19}SC_6H_5$ calculations suggest that adding a top and bottom gold surface will increase the barriers, particularly for ring 3.

If the activation energy of 1.8 kcal/mol deduced from experiment by Reed et al.[2] is indeed related to a rotational barrier and if we assume that an incommensurate herringbone structure is present in the experiments then we can predict that the molecules are perpendicular or close to perpendicular to the surface.

Acknowledgment. A. R. was supported by Contract No. NAS2-03144 to the University Affiliated Research Center (UARC)/UC Santa Cruz. We thank G. Dholakia for helpful discussions.

References and Notes

(1) Chen, J.; Reed, M. A.; Rawlett, A. M.; Tour, J. M. *Science* **1999**, *286*, 1550.

(2) Reed, M. A.; Chen, J.; Rawlett, A. M.; Price, D. W.; Tour, J. M. *Appl. Phys. Lett.* **2001**, *78*, 3735.

(3) Li, C.; Zhang, D.; Liu, X.; Han, S.; Tang, T.; Zhou, C.; Fan, W.; Koehne, J.; Han, J.; Meyyappan, M.; Rawlett, A. M.; Price, D. W.; Tour, J. M. *Appl. Phys. Lett.* **2003**, *82*, 645.

(4) Bauschlicher, C. W.; Ricca, A. *Chem. Phys. Lett.* **2003**, *375*, 459.

(5) Dhirani, A.-A.; Zehner, R. W.; Hsung, R. P.; Guyot-Sionnest, P.; Sita, L. R. *J. Am. Chem. Soc.* **1996**, *118*, 3319.

(6) Yang, G.; Qian, Y.; Engtrakul, C.; Sita, L. R.; Liu, G.-Y. *J. Phys. Chem. B* **2000**, *104*, 9059.

(7) Dholakia, G. R.; Fan, W.; Koehne, J.; Han, J.; Meyyappan, M. *Phys. Rev. B* **2004**, *69*, 153402.

(8) Bauschlicher, C. W.; Ricca, A. *Chem. Phys. Lett.* **2003**, *367*, 90.

(9) Ricca, A.; Bauschlicher, C. W. *Chem. Phys. Lett.* **2003**, *372*, 873.

(10) Stapleton, J. J.; Harder, P.; Daniel, T. A.; Reinard, M. D.; Yao, Y.; Price, D. W.; Tour, J. M.; Allara, D. L. *Langmuir* **2003**, *19*, 8245.

(11) Walzer, K.; Marx, E.; Greenham, N. C.; Less, R. J.; Raithby, P. R.; Stokbro, K. *J. Am. Chem. Soc.* **2004**, *126*, 1229.

(12) Becke, A. D. *J. Chem. Phys.* **1993**, *98*, 5648.

(13) Stephens, P. J.; Devlin, F. J.; Chabalowski, C. F.; Frisch, M. J. *J. Phys. Chem.* **1994**, *98*, 11623.

(14) Hay, P. J.; Wadt, W. R. *J. Chem. Phys.* **1985**, *82*, 299.

(15) Frisch, M. J.; Pople, J. A.; Binkley, J. S. *J. Chem. Phys.* **1984**, *80*, 3265 and references therein.

(16) Frisch, M. J.; Trucks, G. W.; Schlegel, H. B.; Scuseria, G. E.; Robb, M. A.; Cheeseman, J. R.; Montgomery, J. A., Jr.; Vreven, T.; Kudin, K. N.; Burant, J. C.; Millam, J. M.; Iyengar, S. S.; Tomasi, J.; Barone, V.; Mennucci, B.; Cossi, M.; Scalmani, G.; Rega, N.; Petersson, G. A.; Nakatsuji, H.; Hada, M.; Ehara, M.; Toyota, K.; Fukuda, R.; Hasegawa, J.; Ishida, M.; Nakajima, T.; Honda, Y.; Kitao, O.; Nakai, H.; Klene, M.; Li, X.; Knox, J. E.; Hratchian, H. P.; Cross, J. B.; Adamo, C.; Jaramillo, J.; Gomperts, R.; Stratmann, R. E.; Yazyev, O.; Austin, A. J.; Cammi, R.; Pomelli, C.; Ochterski, J. W.; Ayala, P. Y.; Morokuma, K.; Voth, G. A.; Salvador, P.; Dannenberg, J. J.; Zakrzewski, V. G.; Dapprich, S.; Daniels, A. D.; Strain, M. C.; Farkas, O.; Malick, D. K.; Rabuck, A. D.; Raghavachari, K.; Foresman, J. B.; Ortiz, J. V.; Cui, Q.; Baboul, A. G.; Clifford, S.; Cioslowski, J.; Stefanov, B. B.; Liu, G.; Liashenko, A.; Piskorz, P.; Komaromi, I.; Martin, R. L.; Fox, D. J.; Keith, T.; Al-Laham, M. A.; Peng, C. Y.; Nanayakkara, A.; Challacombe, M.; Gill, P. M. W.; Johnson, B.; Chen, W.; Wong, M. W.; Gonzalez, C.; Pople, J. A. *Gaussian 03*, Revision B.03; Gaussian, Inc.: Pittsburgh, PA, 2003.